Natural Carboxylic Acid-Based Deep Eutectic Solvents: Physi-Cochemical Properties, Biological Activities and Application in Flavonoids Extraction from Walnut Green Peel

Lei Gong *, Lili Yue, Qilong Chen, Xuan Liu, Nan Zhang, Jie Zhu

Posted Date: 10 July 2025

doi: 10.20944/preprints202507.0833.v1

Keywords: carboxylic acid-based deep eutectic solvents; physicochemical properties; biological activities; flavonoids

 doi:10.20944/preprints202507.0833.v1

Article

Natural Carboxylic Acid-Based Deep Eutectic Solvents: Physicochemical Properties, Biological Activities and Application in Flavonoids Extraction from Walnut Green Peel

Lei Gong [1,2,*], Lili Yue [2], Qilong Chen [2], Xuan Liu [3], Nan Zhang [2] and Jie Zhu [1]

[1] National-Local Joint Engineering Research Center of Biomass Refining and High-Quality Utilization, Institute of Urban & Rural Mining, Changzhou University, 213164, Jiangsu Province, China.

[2] School of Petrochemical Engineering, Changzhou University, 213164, Jiangsu Province, China.

[3] School of Pharmacy & School of Biological and Food Engineering, Changzhou University, 213164, Jiangsu Province, China.

* Correspondence: gl3007@126.com

Abstract

The development of novel green solvents has become a prominent research focus in the field of green chemistry. Deep eutectic solvents (DESs) have emerged as a promising class of sustainable solvents, offering distinct advantages in terms of cost-effectiveness, tunability, and environmental compatibility. This study presents a systematic investigation of key physicochemical properties, including water content, polarity, conductivity, pH, and viscosity, for ten carboxylic acid-based DESs (CADESs). Furthermore, the antimicrobial efficacy of the investigated CADESs was assessed against representative Gram-positive (*Staphylococcus aureus* and *Enterococcus faecalis*) and Gram-negative (*Escherichia coli* and *Pseudomonas aeruginosa*) bacterial strains. The investigations reveal that CADESs possess broad-spectrum antibacterial activity. The antioxidant properties of the CADESs were systematically evaluated using ABTS and DPPH scavenging assays, and Fe^{2+} chelating activity. Concurrently, phytotoxicity was assessed through germination and early seedling growth tests in mung beans (*Vigna radiata*). Finally, CADESs were used to extract flavonoids from walnut peel. The extraction yield of the Choline chloride/levulinic acid system (containing 30% water) was the highest, reaching 112.8 mg RE·g^{-1} DW. The superior physicochemical properties of CADESs position them as promising green solvents for flavonoids extraction, demonstrating significant potential for widespread application in sustainable technologies.

Keywords: carboxylic acid-based deep eutectic solvents; physicochemical properties; biological activities; flavonoids

1. Introduction

In recent years, Deep Eutectic Solvents (DESs) have garnered increasing attention. Abbott et al. demonstrated that quaternary ammonium salts and amides can form transparent and homogeneous liquids at low temperatures, thereby introducing the concept of eutectic solvents [1]. Natural Deep Eutectic Solvents (NADESs), as an extension of DESs, represent a class of green and sustainable solvents. These solvents typically consist of low-eutectic mixtures formed by the interaction of two or more naturally occurring primary metabolites within organisms (such as organic acids, sugars, amino acids, choline derivatives, etc.) *via* hydrogen-bonding networks [2]. Hydrogen bond acceptors (HBAs) provide hydrogen bond acceptance sites, thereby reducing the melting point of the mixture. Hydrogen bond donors (HBDs), on the other hand, supply protons and establish a hydrogen bond network within the HBAs, disrupting the crystalline structure to achieve eutectic fusion. By

 doi:10.20944/preprints202507.0833.v1

modulating the types, ratios, and interaction patterns of HBAs (e.g., choline, betaine, and amino acids) and HBDs (e.g., sugars, alcohols, amines, and organic acids), NADESs with specific physicochemical properties can be engineered to fulfill diverse application requirements. Owing to their low melting points, low volatility, high biocompatibility, and designable green characteristics, NADESs have emerged as an ideal substitute for conventional organic solvents such as methanol, dimethyl sulfoxide, and chloroform [3]. NADESs successfully address the limitations of Ionic Liquids (ILs) in the extraction of natural products, such as high viscosity, complex synthesis, and poor biocompatibility, by leveraging their adjustable viscosity and green sustainability characteristics. Additionally, NADESs exhibit advantages such as facile preparation and excellent stability. As a significant innovation in the field of green solvents, NADESs have been extensively validated as safe and efficient solvents, showcasing substantial potential in areas including sustainable chemistry, biological extraction, and drug delivery [4]. Especially in the field of natural product extraction, NADESs have attracted significant attention due to their unique solubility and selectivity. Research has demonstrated that HBAs and HBDs in NADESs specifically interact with polar functional groups such as hydroxyl (-OH), glycosidic bonds (-O-), and carboxyl (-COOH) of natural products (e.g., flavonoids, anthocyanins, alkaloids, and glycosides) *via* hydrogen bonding. This interaction disrupts the structure of plant cell walls, thereby facilitating the release of target components [5]. For instance, Chen et al. achieved an extraction yield of 49.41 $mg \cdot g^{-1}$ for total flavonoids from *Rubia cordifolia* using a NADES composed of ChCl and lactic acid. The resulting extract exhibited remarkable antioxidant activity in DPPH, ABTS, and FRAP assays [6]. Zhang et al. developed an efficient and environmentally friendly method for recovering anthocyanins and polyphenols from blueberry pomace by combining ChCl-1,4-butanediol with ultrasonic technology. Their approach demonstrated significantly higher extraction efficiency compared to the use of 70% ethanol [7]. Hou et al. reported that among 16 NADES screening methods, the ultrasound-assisted extraction of saponins from sweet potato roots using ChCl-acrylic acid was the most effective. Furthermore, compared with conventional extraction techniques and molecularly imprinted polymer methods, NADES exhibited a superior extraction rate while maintaining lower costs [8].

Walnut (*Juglans regia*) is a significant economic tree species in China, characterized by a long cultivation history, extensive planting areas, and the highest global production. However, walnut processing has traditionally focused on kernel extraction, leading to the discard or incineration of large quantities of green husks. This practice not only results in resource wastage but also contributes to environmental pollution. Notably, walnut green husks are abundant in bioactive compounds, including flavonoids, naphthoquinones, polyphenols, and terpenoids, which exhibit multiple physiological functions such as antioxidation, anti-tumor activity, and antibacterial properties. As such, walnut green husks are considered an agricultural and forestry waste material with high potential value due to their rich content of bioactive substances [9]. Furthermore, owing to their high mineral content, certain fruit peels are utilized in the production of fertilizers or compost [10]. To date, 13 phenolic compounds have been identified in the extract of walnut green peel, including juglone, caffeic acid, chlorogenic acid, gallic acid, sinapic acid, ferulic acid, ellagic acid, protocatechuic acid, vanillic acid, syringic acid, catechin, myricetin, and epicatechin [11]. Notably, juglone has been recognized for its anti-cancer, antibacterial, and antiviral properties [12].

Flavonoids, a class of polyphenolic compounds, are ubiquitously distributed throughout the plant kingdom, from roots to fruits. To date, over 8,000 distinct flavonoid structures have been characterized [13]. These natural products exhibit substantial biological activities, such as antiviral, anti-allergic, lipid-lowering, antibacterial, and anti-inflammatory effects, as well as the potential to prevent cardiovascular and cerebrovascular diseases. Additionally, they serve as natural colorants and antioxidants in the food industry [14]. Due to the complexity and diversity of their structures, flavonoids pose a challenge in identifying a universal method for extraction from various plant sources. Currently, organic solvents such as methanol, ethanol, and ethyl acetate are commonly employed as media for flavonoid extraction; however, these traditional methods exhibit notable limitations [13,15]. From a technological standpoint, the operational process is relatively complex,

 doi:10.20944/preprints202507.0833.v1

encompassing numerous processing stages and typically necessitating high-temperature conditions to complete the extraction. In terms of efficiency, this method not only consumes substantial amounts of organic solvents but also entails a prolonged extraction cycle, which is both time-consuming and labor-intensive. Regarding the analysis of extraction outcomes, organic solvents are prone to inducing ionization, hydrolysis, or oxidation reactions in flavonoids, potentially leading to the loss of their biological activity. From the perspectives of environmental protection and safety, certain organic solvents may cause significant environmental pollution and simultaneously pose potential risks to human health. Given the limitations of traditional organic solvents in the flavonoid extraction process, Natural carboxylic acid-based deep eutectic solvents (CADESs) exhibit unique application potential. Through precise screening and formulation of appropriate components, CADESs can significantly enhance the solubility of target flavonoids and markedly improve extraction efficiency. Notably, CADESs can achieve the simultaneous extraction of multiple compounds with significant property differences. By optimizing separation conditions, efficient separation can be achieved, thus establishing a novel pathway for green and efficient flavonoid extraction and demonstrating substantial application potential and promising development prospects [16–18]. However, with a focus on the walnut green peel, a raw material possessing potential medicinal and functional component value, the current research on the extraction process of CADESs remains relatively limited. In comparison to the investigation of other extraction media or DES types for the extraction of walnut green peels, the DES system based on natural carboxylic acids has yet to be fully explored.

In this study, we systematically designed and synthesized a series of CADESs based on choline chloride and natural renewable carboxylic acids (as shown in Figure 1). A comprehensive investigation was conducted on their physicochemical properties, antibacterial capabilities, antioxidant characteristics, and phytotoxicity. Additionally, the flavonoids extracted from green walnut husks were evaluated using the prepared CADESs.

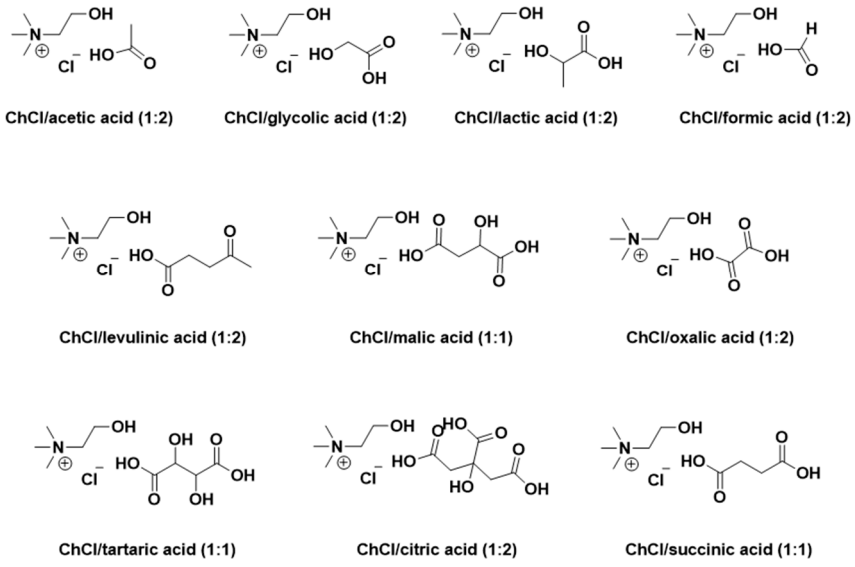

Figure 1. Structure of CADESs based on choline chloride (ChCl).

2. Results and Discussion

2.1. Physicochemical Properties

The physicochemical properties displayed by different compositions of CADESs vary significantly, including factors such as moisture content, polarity, conductivity, pH, and viscosity. The determination results were presented in Table 1 and Figure 2.

 doi:10.20944/preprints202507.0833.v1

2.1.1. Moisture Content

Due to the influence of factors such as the inherent moisture content of raw materials and environmental moisture infiltration during the synthesis process, the prepared CADES inevitably contain a certain level of moisture. The moisture content of CADES exerts a profound impact on their physicochemical properties, with viscosity and electrical conductivity being particularly sensitive indicators. Typically, an increase in moisture content leads to a corresponding decrease in the viscosity of CADES. This behavior can be attributed to the dilution effect of water molecules, which disrupts the intermolecular interactions, including hydrogen bonds and van der Waals forces, within the CADES matrix [19]. By reducing the cohesive forces between the components, water enhances the fluidity of the system.

In this study, the moisture content of the ten prepared CADES samples varied significantly, ranging from 1.3% to 30.2%. Notably, an optimal moisture level can substantially enhance the electrical conductivity of CADES. Due to their high polarity, water molecules facilitate the dissociation and migration of ions or polar species within the CADES, thereby enhancing the charge-carrying capacity of the system [20]. Experimental results demonstrate that CADES formulations such as CADES-1(30.2% moisture), CADES-5 (27.0% moisture), and CADES-7 (19.3% moisture) exhibit significantly higher electrical conductivity compared to their low-moisture counterparts. These findings provide strong empirical evidence for the positive correlation between moisture content and electrical conductivity in CADES systems.

2.1.2. Polarity

The polarity of these solvents is quantitatively characterized by the molar transition energy (E_{NR}) [21]. The values of E_{NR} span from 47.8 for CADES-2, while glycolic acid serves as the HBD, to 93.4 for CADES-6, which employs malic acid as the HBD. These results strongly suggest that strong hydrogen-bonding and dipole interactions are the defining features of these CADESs. Furthermore, the carboxyl groups of oxalic acid interact with the quaternary ammonium cations of choline chloride through hydrogen bonding and electrostatic attraction. Meanwhile, there is both electrostatic repulsion and attraction between oxalate anions and chloride ions. This intricate interplay of forces leads to a more uneven charge distribution within the system, thereby significantly enhancing the polarity of the CADES. Similarly, the carboxyl and hydroxyl groups of malic acid also engage in analogous interactions with choline chloride. As a result of these robust intermolecular interactions and the subsequent charge-distribution effects, CADESs composed of choline chloride with oxalic acid or malic acid exhibit the highest polarity among the tested systems.

2.1.3. Conductivity

CADES with diverse compositions, characterized by different HBDs, exhibit distinct ionization degrees and ion mobilities, thereby giving rise to significant variations in electrical conductivity. For instance, the CADES formulated from choline chloride and oxalic acid demonstrates a notably high conductivity value of 21300 $\mu S \cdot cm^{-1}$. In stark contrast, the DES, composed of choline chloride and citric acid, shows a much lower conductivity, registering at only 4.79 $\mu S \cdot cm^{-1}$. This disparity underscores the critical role of the HBD in determining the ionic properties and, consequently, the electrical conductivity of CADES systems. Higher moisture content CADES generally have higher electrical conductivity. The ability of water molecules to enhance ion mobility and facilitate ionic dissociation within the CADES matrix accounts for this phenomenon [22].

2.1.4. pH

CADES generally feature a low pH, endowing them with distinct acidic properties. This characteristic significantly boosts the solubility of flavonoids, as these compounds tend to be more stable in acidic media. In an acidic environment, flavonoid molecules undergo protonation, which disrupts intermolecular forces, facilitating better dispersion within the solvent matrix [23].

 doi:10.20944/preprints202507.0833.v1

Additionally, the acidic conditions of CADES suppress the degradation pathways of flavonoids. By reducing the activity of degradation-inducing enzymes and inhibiting certain chemical reactions, the solvent effectively retards the decomposition of flavonoids. This dual effect not only enhances the solubility of flavonoids but also preserves their structural integrity, ensuring their prolonged stability within the CADES system.

Table 1. Physicochemical properties of CADESs.

Number	CADESs	Moisture content (wt%)	Polarity (kcal·mol^{-1})	Conductivity (μs·cm^{-1})	pH
CADES-1	ChCl/acetic acid	30.2	48.2	4880	1.11
CADES-2	ChCl/glycolic acid	1.5	47.8	2110	0.10
CADES-3	ChCl/levulinic acid	2.1	48.6	965	1.28
CADES-4	ChCl/lactic acid	7.3	48.1	1986	0.76
CADES-5	ChCl/formic acid	27.0	48.1	15930	0.14
CADES-6	ChCl/malic acid	1.3	93.4	66.8	1.7
CADES-7	ChCl/oxalic acid	19.3	92.2	21300	1.4
CADES-8	ChCl/tartaric acid	5.0	48.1	281	1.7
CADES-9	ChCl/citric acid	7.4	79.9	4.79	1.4
CADES-10	ChCl/succinic acid	2.5	47.9	1411	1.7

2.1.5. Viscosity

The viscosity of CADES increases with the strength of intermolecular hydrogen bonding [24]. As clearly illustrated in Figure 2, CADES 6-10 exhibits a relatively high viscosity. This can be attributed to its HBD, which is a polycarboxylic acid. Upon forming DES with choline chloride, a compound known for its strong hydrogen bond acceptor capability, the multiple carboxyl groups of the polycarboxylic acid establish an extensive network of hydrogen bonds with choline chloride. Consequently, this interaction results in the relatively high viscosity observed in this DES. Generally, as the length of the carbon chain increases, the volume of the polycarboxylic acid molecule also increases, leading to a corresponding increase in van der Waals forces between the molecules. Additionally, longer carbon chains enhance molecular flexibility, which complicates the entanglement and interactions between molecules. This results in an increase in the viscosity of CADES. For example, succinic acid has a longer carbon chain compared to oxalic acid, and consequently, the viscosity of CADES prepared using succinic acid as a raw material tends to be relatively higher. In addition, Conversely, branched structures in polycarboxylic acids introduce steric hindrance, increasing the distance between molecules. This impairs hydrogen bond formation and disrupts close molecular packing, leading to a decrease in CADES viscosity. Consequently, this effect contributes to a reduction in the viscosity of CADES. For example, the viscosity of CADES formed by succinic acid is higher compared to that formed by tartaric acid and malic acid. Moreover, temperature exerts a profound influence on the viscosity of CADES. As the temperature rises, the increased molecular thermal motion intensifies, effectively weakening the intermolecular forces [25,26]. Consequently, the resistance to molecular flow diminishes, leading to a notable decrease in viscosity.

 doi:10.20944/preprints202507.0833.v1

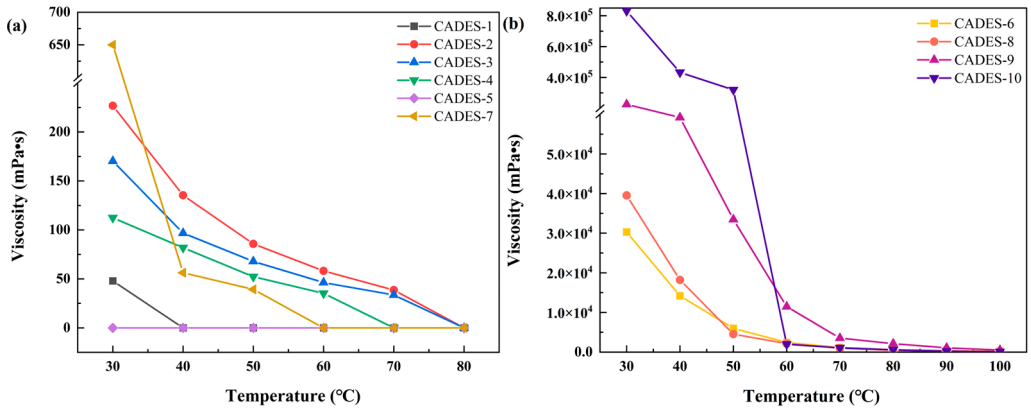

Figure 2. Effect of temperature on the viscosity of CADESs.

2.2. Antioxidant Property

2.2.1. DPPH Radical Scavenging Activity

Due to the high viscosity of CADES 6-10, which may impede the accurate determination of their antioxidant activity, all samples in this group were uniformly diluted 20-fold prior to antioxidant activity assessment. The results were summarized in Table 2. Our study revealed that several low-viscosity CADES 1-5 demonstrate comparable DPPH radical scavenging rates. Despite variations in specific intermolecular interactions, these solvents exhibit similar reactivity and contact efficiency between active sites and DPPH radicals under low-viscosity conditions, resulting in closely aligned DPPH radical scavenging efficiencies. This finding suggests that within the CADES systems characterized by similar structural features (such as monocarboxyl functional groups) and good fluidity, the reaction mechanisms and efficiencies with DPPH radicals are relatively consistent, thereby yielding comparable DPPH test results. From the perspective of functional group chemistry, the hydroxyl group (-OH), a quintessential active hydrogen donor, can directly reduce DPPH radicals through the hydrogen atom transfer (HAT) mechanism [27]. Notably, in CADES-6, CADES-8, and CADES-10, a linear correlation was observed between the number of hydroxyl groups in the molecular structure and the free radical scavenging efficiency. Additionally, CADES-7, with its unique spatial configuration and strong polarity, exhibits distinct advantages in radical scavenging. Even after a 20-fold dilution, this system maintains an impressive DPPH radical scavenging rate of 85.2%, highlighting its exceptional antioxidant capacity.

2.2.2. ABTS Radical Scavenging Activity

As detailed in Table 2, the CADES systems formulated with different carboxylic acids as HBDs demonstrate distinct ABTS radical scavenging efficiencies. In the ABTS antioxidant test, differences in the number and spatial distribution of active groups, such as carboxylic acid and hydroxyl groups, were found to have a significant effect on antioxidant performance. Carboxylic acids containing conjugated structures or multiple adjacent hydroxyl groups, such as acetylpropionic acid or tartaric acid, exhibit enhanced hydrogen dissociation due to conjugation effects or intramolecular hydrogen bonding, resulting in relatively high antioxidant activity in the ABTS test. Conversely, CADES formed from linear saturated carboxylic acids display relatively weaker antioxidant activity, such as formic acid and acetic acid. This phenomenon can be primarily attributed to the conjugation effect and intramolecular hydrogen bonding [28].

2.2.3. Fe^{2+} Chelating Activity

As illustrated in Table 2, the chelating capabilities of carboxylic acids with diverse structures towards Fe^{2+} exhibit substantial disparities. Oxalic acid, owing to its unique molecular architecture, emerges as an exemplary ligand for Fe^{2+}. The adjacent positioning of its two carboxyl groups offers

 doi:10.20944/preprints202507.0833.v1

precisely aligned coordination sites, enabling a highly efficient interaction with Fe^{2+} ions [29]. Upon complexation, the two carboxyl oxygen atoms of oxalic acid simultaneously form coordination bonds with a single Fe^{2+} ion, giving rise to a stable five-membered ring chelate. The minimal ring strain inherent to five-membered structures endows this configuration with exceptional spatial stability. Furthermore, the formation of these coordination bonds triggers electron cloud redistribution between Fe^{2+} and oxalic acid, further augmenting the overall stability of the chelate complex. During this process, choline chloride acts as a hydrogen bond acceptor, interacting via hydrogen bonding with oxalic acid molecules. This interaction modulates the electron cloud environment surrounding oxalic acid, aligning the electron density distribution of the carboxyl oxygen atoms more closely with the coordination requirements of Fe^{2+}, thus significantly promoting the chelation reaction and enhancing the capture and stabilization of Fe^{2+}. In contrast, the chelating ability of glycolic acid with Fe^{2+} differs markedly from that of oxalic acid due to its distinct structural characteristics and coordination mechanism. Both the carboxyl and hydroxyl groups in glycolic acid are active and capable of coordinating with Fe^{2+}. Specifically, the oxygen atom in the hydroxyl group forms a coordination bond with the empty orbital of Fe^{2+} through its lone pair of electrons, while the carboxyl group participates in the chelation reaction via conventional carboxyl-oxygen coordination. When interacting with Fe^{2+}, glycolic acid molecules can adopt multiple coordination modes with flexibility, thereby forming stable and diverse chelating structures that effectively bind Fe^{2+}. In comparison to certain other carboxylic acid-based deep eutectic solvents, some systems exhibit limited coordination sites due to an insufficient number or suboptimal distribution of active groups within the carboxylic acid molecules, which hinders efficient Fe^{2+} chelation. Consequently, in terms of Fe^{2+} chelating capacity, these systems are significantly inferior to the choline-oxalic acid and choline-glycolic acid systems.

Table 2. Antioxidant properties of CADESs.

Number	CADESs	DPPH（%）	ABTS（%）	Fe^{2+}（%）
CADES-1	ChCl/acetic acid	96.2±3.3	14.1±3.8	13.2±3.2
CADES-2	ChCl/glycolic acid	97.1±3.2	16.0±1.1	98.9±0.4
CADES-3	ChCl/levulinic acid	96.1±1.0	30.4±2.4	49.6±3.0
CADES-4	ChCl/lactic acid	95.0±0.7	35.2±3.1	85.1±0.6
CADES-5	ChCl/formic acid	95.4±2.0	6.6±3.4	87.9±0.1
CADES-6*	ChCl/malic acid	53.4±0.8	16.4±1.3	8.3±0.5
CADES-7*	ChCl/oxalic acid	85.2±0.4	14.8±1.1	96.2±2.0
CADES-8*	ChCl/tartaric acid	55.0±0.1	19.2±1.9	8.4±1.3
CADES-9*	ChCl/citric acid	46.4±2.1	13.8±1.5	7.1±1.1
CADES-10*	ChCl/succinic acid	38.2±0.8	9.6±0.9	2.9±1.0

*CADES-6~10: 20-fold dilution with water.

2.3. Antibacterial Property

2.3.1. Antibacterial Zone

The antibacterial activities of ten CADESs against *Staphylococcus aureus* (*S. aureus*), *Enterococcus faecalis* (*E. faecalis*), *Escherichia coli* (*E. coli*), and *Pseudomonas aeruginosa* (*P. aeruginosa*) were investigated. The filter paper diffusion method (Figure 3) was employed to assess the antibacterial performance, with the diameter of the inhibition zones serving as the key indicator, as demonstrated by ChCl-glycolic acid (Figure S1). The findings revealed that all tested CADES demonstrated antibacterial effects to varying extents. Notably, the efficacy of these CADES was significantly influenced by both the specific type of CADES and the targeted bacterial species. Notably, the

 doi:10.20944/preprints202507.0833.v1

CADES-5 exhibits potent antibacterial properties, particularly pronounced inhibitory effects on *P. aeruginosa* and *E. faecalis*. The exceptional activity can be attributed to the low molecular weight and lipophilic properties of formic acid, enabling it to penetrate bacterial cell membranes efficiently. Once inside the cells, formic acid disrupts cellular metabolic pathways, thereby impeding bacterial growth and reproduction. In contrast, the CADES-7 exhibits the highest level of antibacterial activity against *S. aureus* and *E. coli*. The exceptional chelating capability of oxalic acid toward metal ions is a key contributing factor. By binding to metal ions essential for bacterial growth, oxalic acid prevents their participation in cellular metabolism or coenzyme functions, thus disrupting normal bacterial physiological processes and exerting its antibacterial effects. These findings align with recent studies on the antibacterial mechanisms of CADES, suggesting that its antibacterial activity is closely associated with its low pH value, hydrogen bond donor characteristics, and its destructive impact on bacterial cell membranes [30–32]. Furthermore, considering the environmental friendliness and low toxicity of CADES, its potential application value in the field of antibacterial agents merits further investigation [33,34].

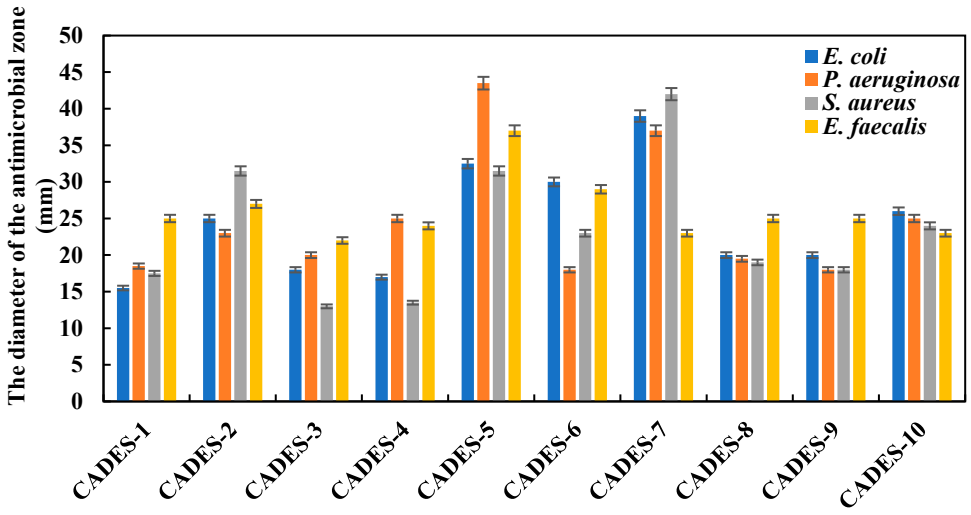

Figure 3. Inhibition of bacteria in Petri dishes by different CADESs.

2.3.1. The MIC of CADESs

In the study of the inhibitory effects of CADESs on microorganisms, the minimum inhibitory concentration (MIC) is a crucial parameter for assessing the potency of these solvents [35]. It accurately represents the lowest concentration needed to halt microbial growth. As shown in Table 3, CADES-5 stands out among various CADESs, displaying the lowest MIC value (MIC=3.75 mg·mL^{-1}) against the four tested microbial strains. Structural analysis reveals that formic acid possesses a relatively small molecular size and moderate lipid solubility, which confers choline-formic acid chloride with distinctive antibacterial properties. Upon interaction with microorganisms, the lipophilic nature of formic acid enables it to efficiently penetrate bacterial cell membranes and disrupt essential metabolic processes within the cell, such as inhibiting energy synthesis pathways or interfering with the biosynthesis of proteins and nucleic acids, thereby effectively suppressing microbial proliferation. Conversely, other CADESs, such as CADES-1, exhibit larger molecular dimensions due to the additional methyl group in acetic acid. This results in reduced efficiency in penetrating bacterial cell membranes compared to formic acid, necessitating higher concentrations to achieve equivalent antibacterial effects, as reflected by elevated MIC values. Additionally, the observed antibacterial efficacy aligns with the trends in the diameters of the antibacterial zones.

 doi:10.20944/preprints202507.0833.v1

Table 3. Toxicity of CADESs to bacteria, expressed as MIC (mg·mL^{-1}).

CADESs	*E. coli*	*P. aeruginosa*	*S. aureus*	*E. faecalis*
ChCl/acetic acid	7.5	3.75	7.5	7.5
ChCl/glycolic acid	7.5	7.5	15	7.5
ChCl/levulinic acid	7.5	7.5	15	15
ChCl/lactic acid	30	30	15	30
ChCl/formic acid	3.75	3.75	3.75	3.75
ChCl/malic acid	15	7.5	30	30
ChCl/oxalic acid	7.5	7.5	7.5	7.5
ChCl/tartaric acid	30	15	15	15
ChCl/citric acid	15	7.5	7.5	15
ChCl/succinic acid	15	15	15	15

2.4. The CADES on the Germination Toxicity of Mung Beans

The change in water content significantly affects the interaction mode between CADES and biomolecules such as proteins and nucleic acids, thereby altering their transmembrane transport efficiency and in vivo metabolic pathways [36]. When exploring the effect of CADES on the germination of plant seeds, CADES with different water contents exhibit differential regulatory effects, either promoting or inhibiting the seed germination process. For instance, in the case of choline chloride-succinic acid, the corresponding effect profile based on experimental measurements was illustrated in Figure S2.

When CADES exists in a high-concentration state, a hypertonic environment will be formed around the seeds. Since the water potential inside the mung bean seeds is higher than that of the external solution, the water flows in the reverse direction, resulting in the seeds being unable to absorb sufficient water to initiate the germination program, thus significantly delaying or inhibiting seed germination. In sharp contrast, low-concentration CADES can stimulate the germination of mung bean seeds, effectively enhance seed vitality, and strengthen the internal physiological and metabolic activities. The experimental data in Table 4 indicated that within a reasonable concentration range, as the dilution multiple of CADES increases, its promoting effect on mung bean germination gradually enhances; however, when the concentration is too high, the inhibitory effect will appear sharply. Multiple systems, such as choline chloride-lactic acid, choline chloride-levulinic acid, and choline chloride-formic acid, all exhibit the typical concentration response characteristics of "inhibition at high concentration and promotion at low concentration".

It is worth noting that choline chloride-oxalic acid shows a strong inhibitory effect on the germination of mung beans. Even under the condition of 400-fold high dilution, the inhibitory effect is still significant: on the fourth day of treatment, the shoot length is only 0.3 mm, and the RGP% is as low as 20%. This phenomenon is mainly due to the strong metal chelating ability endowed by the special dicarboxylic acid structure of oxalic acid [37]. During the seed germination process, oxalic acid can efficiently chelate calcium ions (Ca^{2+}) in the endosperm. Since Ca^{2+} is a key cofactor for the activity of many enzymes, the change in its concentration and distribution directly interferes with the normal function of Ca^{2+}-dependent enzymes, blocking the key physiological and biochemical reactions required for seed germination.

In contrast, under the condition of 2000-fold low-concentration dilution, choline chloride-tartaric acid and choline chloride-formic acid show a significant promoting effect on the germination of mung bean. Compared with the deionized water control group, the shoot lengths increased by 34.7 mm and 32.8 mm, respectively. Although CADES is usually composed of natural compounds, previous studies generally believe that it has good biological safety, and there are few reports on its toxicity [38]. Moreover, toxicological evaluations have not been carried out in most application fields. This

 doi:10.20944/preprints202507.0833.v1

study provides important theoretical basis and data support for the safe application of CADES as a green solvent in the agricultural field by establishing a phytotoxicity evaluation system.

Table 4. Toxic effects of CADESs on mung bean germination.

Solvents	Dilution factor	Number of days (bud length: mm)				RGP %
		1 day	2 days	3 days	4 days	
Deionized water	/	6.5	21.8	27.1	41.5	100
ChCl/acetic acid	400	1.4	9.4	13.1	14.6	60
	1200	5	25.5	33.5	35.2	90
	2000	2.7	15.8	30.6	29.7	100
ChCl/glycolic acid	400	3.6	13.5	20.9	22.7	100
	1200	7.4	23.5	35.7	37.6	90
	2000	2.3	17.7	31.5	34.2	100
ChCl/levulinic acid	400	1.9	3.2	3.8	3.4	100
	1200	4.9	11.5	15.5	23.7	100
	2000	7.1	22.1	35.8	60	100
ChCl/lactic acid	400	6.2	13.6	19.8	31.1	100
	1200	7.7	23.4	40.3	52	100
	2000	9.4	28.1	45.8	65.6	100
ChCl/formic acid	400	2.6	3.4	7.2	7.8	100
	1200	8.9	20.3	35.7	54.8	100
	2000	7.5	23.8	62.4	74.3	100
ChCl/malic acid	400	7.8	19.1	25.4	25.6	100
	1200	8.2	24.3	31.5	32.3	100
	2000	10.6	26.2	36.1	40.2	100
ChCl/oxalic acid	400	0	0.3	0.3	0.3	20
	1200	2.7	7.7	12.3	12.8	100
	2000	7.8	28.3	40.3	41.5	100
ChCl/tartaric acid	400	1.8	2.8	3.4	3.4	100
	1200	4	12.3	23.3	33.3	100
	2000	5.9	15.4	33.8	57.7	100
ChCl/citric acid	400	4.5	12.4	17.3	19.9	100
	1200	4.7	16.4	25.9	42.1	100
	2000	7.1	26.3	52.2	69	100
ChCl/succinic acid	400	3.3	6	9.6	12.8	100
	1200	9.1	22.4	51.9	71.1	100
	2000	8.3	27.7	49.5	76.2	100

2.5. Extract Flavonoids from Walnut Green Peel Using CADESs

As depicted in Figure 4, notable discrepancies are observed in the extraction efficiencies of flavonoids from walnut green peel when different carboxylic acid-based deep eutectic solvents (DESs) are employed. The extraction yields vary significantly, spanning from 48.6 to 112.8 mg RE·g^{-1} DW. This extraction approach primarily operates by disrupting the plant cell wall structure. By capitalizing on the acidic properties of carboxylic acids, it hydrolyzes cell wall components, effectively enhancing cellular permeability and facilitating the dissolution of flavonoids. Furthermore, CADES can form stable complexes with flavonoids via non-covalent interactions such as hydrogen bonding, effectively extracting them from plant matrices [39]. Notably, the extraction efficiency of this method generally outperforms that of traditional techniques. For instance, when extracting walnut green peel using choline-acetylpropionic acid containing 30% water at 50 °C for 1 h, the total flavonoid content reaches 112.8 mg RE·g^{-1} DW. In contrast, extraction with 70% ethanol yields only 37.7 mg RE·g^{-1} DW, reflecting an approximately threefold enhancement in extraction efficiency. The superior flavonoid extraction performance of choline chloride-acetylpropionic acid is

 doi:10.20944/preprints202507.0833.v1

primarily attributed to π-π stacking interactions between the ketone group structure within the acetylpropionic acid molecule and flavonoids. These interactions strengthen the affinity between the solvent and target compounds while reducing the binding energy of flavonoids within plant cells, thereby promoting their separation from plant tissues and entry into the solvent system, which significantly enhances extraction efficiency [40].

CADESs offer several notable advantages, including easy accessibility of raw materials, low cost, minimal toxicity, and environmental friendliness. They enable efficient extraction under relatively mild conditions, eliminating the need for extreme factors such as high temperature or pressure [41,42]. These characteristics highlight their substantial potential for industrial applications.

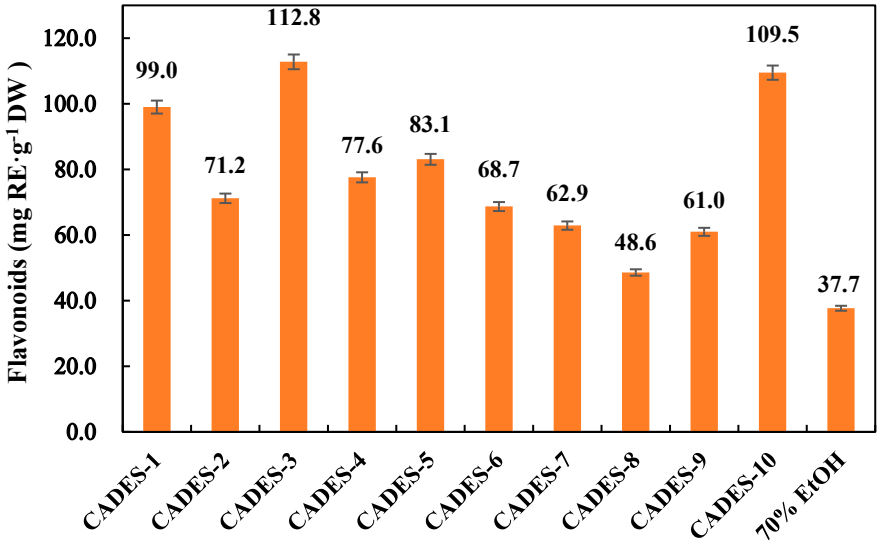

Figure 4. Effect of different CADESs on flavonoids extraction from walnut green peel.

3. Materials and Methods

3.1. Chemicals

Choline chloride, acetic acid, formic acid, sodium hydroxide, sodium nitrite, and 2,2-diphenyl-1-picrylhydrazyl (DPPH) were procured from Shanghai Maclin Biochemical Technology Co., Ltd. Rutin, anhydrous ethanol and aluminum nitrate were obtained from Shanghai Aladdin Biochemical Technology Co., Ltd. Lactic acid, citric acid, and oxalic acid dihydrate were sourced from Sinopharm Group Chemical Reagent Co., Ltd. All other chemicals were used as received without further purification. The fresh walnut green peel samples were collected from Longling County, Baoshan City, Yunnan Province, China. Following collection, the samples underwent manual peeling, were air-dried at room temperature, mechanically crushed, and sieved through standard mesh filters. The processed materials were then stored in airtight containers at 4 °C for subsequent experimental use.

3.2. Preparation of CADESs

In this research, ten carboxylic acid-based CADESs were successfully synthesized. Choline chloride (ChCl) was employed as HBA, which was meticulously combined with various carboxylic acids (functioning as HBDs) at precisely defined molar ratios [43]. These mixtures were subjected to heating while being continuously stirred until uniform, transparent liquids were formed, as illustrated in Figure 5. Owing to their high degree of purity, the synthesized CADESs did not necessitate additional purification steps. They were subsequently stored in glass vials at ambient temperature, ready for use in subsequent experimental procedures.

 doi:10.20944/preprints202507.0833.v1

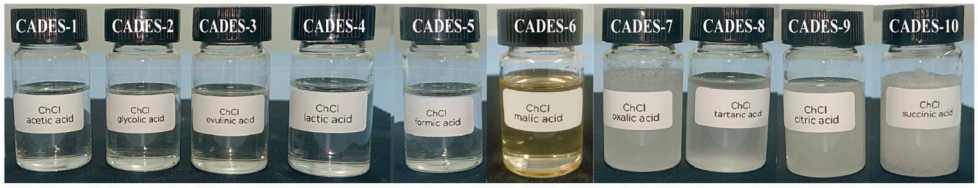

Figure 5. Room temperature state of CADESs.

3.3. Physicochemical Properties

3.3.1. pH Measurement

The pH values of the CADES were determined using a calibrated digital pH meter (PHS-25, Inesa Scientific Instrument Co., LTD, China) equipped with a high-temperature-resistant composite electrode. To guarantee measurement accuracy, a two-point calibration was initially carried out using standard buffer solutions (pH 4.00 and 6.86). For CADES-1 to CADES-6, the pH measurements were conducted at 25 °C under ambient conditions. In contrast, for CADES-7 to CADES-10, which necessitated elevated-temperature characterization, the measurements were executed at 80 °C. Before these measurements, both the samples and pH calibration buffers were preheated to the target temperature of 80 °C. The pH value was recorded only after the meter reading had stabilized, ensuring reliable and accurate data collection.

3.3.2. Electrical Conductivity Determination

The electrical conductivity of CADESs was measured using a calibrated conductivity meter (DJS-1VTC, Inesa Scientific Instrument Co., LTD, China) equipped with a temperature-compensated electrode. Before measurements, the instrument was standardized with a 0.01 mol·L^{-1} KCl reference solution at the corresponding measurement temperatures to ensure data accuracy. The Samples were analyzed under two temperature conditions: CADES-1 to CADES-6 were measured at a constant temperature of 25 °C, while CADES-7 to CADES-10 underwent measurements at an elevated temperature of 80 °C. For the high-temperature measurement group, both the buffer solution and the sample were preheated simultaneously to the target temperature of 80 °C before the experiment commenced. A specialized high-temperature composite electrode was employed for these measurements. The conductivity value was recorded only after the instrument reading had stabilized, guaranteeing the acquisition of precise and reliable data.

3.3.3. Viscosity Determination

The viscosity characteristics of CADES under different temperature conditions were determined using a digital rotational viscometer (NDJ-1C, Shanghai Fangrui Instrument Co., LTD, China). The experimental protocol was conducted as follows: precisely 20 mL of CADES was measured and transferred into a specialized circular flat-bottomed measuring vessel. An appropriate measuring rotor was selected according to the estimated viscosity range of the sample (rotor 21# for 500-100,000 mPa·s; rotor 27# for 2,500-500,000 mPa·s; rotor 28# for 5,000-1,000,000 mPa·s; rotor 29# for 10,000-2,000,000 mPa·s), with careful attention paid to ensure complete submersion of the rotor beneath the liquid surface. Subsequently, the CADES sample was gradually heated to predetermined test temperatures (30-100 °C) using a precision temperature control system. Once the temperature had stabilized at each target point, the viscosity values of the CADES were systematically recorded and measured.

3.3.4. Moisture Content Determination

The moisture content determination procedure commenced with the precise weighing of a clean, dry conical flask; its mass was recorded as m_1. Subsequently, the CADES sample was carefully

 doi:10.20944/preprints202507.0833.v1

transferred into the flask, and the combined mass of the flask and sample was measured and recorded as m_0. The conical flask, now containing the CADES sample, was placed in a conventional oven set at 105 °C under ambient pressure. This initial drying step, which lasted for 2 h, aimed to evaporate the majority of free moisture within the sample. Following this, the sample was transferred to a vacuum drying oven maintained at 70 °C. The drying process continued under vacuum conditions until a constant mass was reached, indicating complete removal of residual moisture. The final mass of the dried sample and flask was recorded as m. The moisture content (%) within the CADES sample was calculated using the following formula:

$$\text{Moisture Content}(\%) = \frac{m0 - m}{m0 - m1} \times 100 \quad (1)$$

Among these, m_0 represents the total mass (g) of the CADES and the conical flask before the drying process; m_1 denotes the mass (g) of the empty conical flask; and m indicates the total mass (g) of the CADES and the conical flask after the completion of the drying procedure.

3.3.5. Polarity Determination

The polarity of CADES was determined following the solvatochromic method developed by Watanabe, Ogihara, and colleagues [44], with Nile red employed as the polarity-sensitive probe. The experimental protocol was executed as follows: Initially, 10.0 mg of Nile red dye was precisely weighed and dissolved in anhydrous ethanol to prepare a 1.0 mg·mL^{-1} stock solution, which was stored protected from light at 4 °C to prevent photodegradation. Immediately before each analysis, the stock solution was diluted 100-fold with anhydrous ethanol, yielding a 10 μg·mL^{-1} working solution. For the polarity measurement, 900 μL of the Nile red working solution was mixed with 7.2 mL of CADES. The resulting mixture was then kept in the dark for 10 min to ensure the establishment of solvation equilibrium. UV-Vis spectrophotometric analysis was carried out, using the corresponding CADES (devoid of Nile red) as the blank reference. The absorption spectrum was recorded within the 400-700 nm range to accurately identify the maximum absorption wavelength (λ_{max}). Finally, the molar transition energy (E_{NR}) was calculated *via* formula (2), serving as a quantitative indicator of the solvent polarity.

$$E_{NR}\ (\text{kcal/mol}) = \frac{28591}{\lambda_{max}} \quad (2)$$

3.4. Antioxidant Activity

3.4.1. DPPH Radical Scavenging Activity

The antioxidant capacity of CADES was evaluated using the 2,2-diphenyl-1-picrylhydrazyl (DPPH) radical scavenging assay, adhering to the standardized protocol developed by Sarikurkcu et al. [45]. Briefly, a 0.05 mg·mL^{-1} DPPH working solution was freshly prepared by precisely weighing DPPH and dissolving it in anhydrous ethanol. This solution was protected from light and used immediately to ensure optimal radical activity. In the assay procedure, 2 mL of the CADES sample or 20-fold diluted CADES was combined with 2 mL of the DPPH solution. The mixture was vigorously vortexed to ensure complete homogenization, followed by incubation at room temperature in the dark for 2 h. After incubation, the absorbance of the reaction mixture was measured at 517 nm using a UV-Vis spectrophotometer. The results were calculated according to formula (3) and presented in the form of the percentage of cleared DPPH free radicals.

$$\text{DPPH scavenging rate}\ (\%) = [\,1 - \frac{(A1 - A2)}{A0}\,] \times 100 \quad (3)$$

Among these, A_0 denotes the absorbance of the control group, which consists of the DPPH solution without the presence of CADESs; A_1 represents the absorbance of the reaction solution containing both CADES and DPPH; and A_2 signifies the absorbance of the CADES sample in the absence of the DPPH solution.

 doi:10.20944/preprints202507.0833.v1

3.4.2. ABTS Radical Scavenging Activity

The ABTS radical scavenging capacity of CADES was evaluated using a method adapted from Jia et al. [46]. The experimental protocol was carried out as follows: Initially, 38.4 mg of 2,2′-azino-bis(3-ethylbenzothiazoline-6-sulfonic acid) (ABTS) and 6.6 mg of $K_2S_2O_8$ were precisely weighed and dissolved in 20 mL of deionized water. The resulting mixture was shielded from light and allowed to react at room temperature for 12 h to generate the ABTS radical cation ($ABTS^{\cdot+}$) stock solution. Subsequently, the $ABTS^{\cdot+}$ stock solution was diluted with anhydrous ethanol until its absorbance at 734 nm reached 0.70±0.02. This working solution was freshly prepared for each experiment run to ensure consistency and accuracy. For the assay, 2 mL of the CADES sample was mixed with 6 mL of the $ABTS^{\cdot+}$ working solution. The mixture was then vortexed thoroughly to ensure complete homogenization and incubated at room temperature in the dark for 10 min. After the incubation period, the absorbance of the mixture was measured at 734 nm using a UV-Vis spectrophotometer. The ABTS radical scavenging activity was calculated according to formula (4) and expressed as a percentage of radical inhibition.

$$\text{ABTS scavenging effect (\%)} = [1- \frac{(As- Ab)}{Ac}] \times 100 \quad (4)$$

Among these, A_c represents the absorbance of the control group, which is the ABTS solution without the addition of CADES; A_s denotes the absorbance of the reaction solution containing both CADES and ABTS; and A_b signifies the absorbance of the CADES sample in the absence of the ABTS solution.

3.4.3. Fe^{2+} Chelating Activity

Under acidic conditions, Fe^{2+} ions react with Ferrozine to form a stable purple-colored complex that exhibits maximum absorbance at 562 nm, as reported in previous literature [47]. The experimental protocol is conducted as follows: First, precisely pipette 2 mL of CADES, 5.46 mL of deionized water, and 140 μL of $FeSO_4$ solution (2 mmol·L^{-1}) into a test tube, followed by vigorous vortex mixing. Subsequently, 400 μL of a 5 mmol·L^{-1} Ferrozine solution was added, and the mixture was thoroughly agitated again. To facilitate complete complex formation, the reaction mixture was incubated in the dark at room temperature for 20 min. Finally, the absorbance of the resulting solution was measured at 562 nm using a spectrophotometer, and the Fe^{2+}-free radical scavenging activity was calculated according to formula (5), with results presented as the percentage scavenging activity.

$$Fe^{2+} \text{ scavenging rate (\%)} = [\ 1- \frac{(A4- A5)}{A3}\ ] \times 100 \quad (5)$$

Among these, A_3 represents the absorbance of the control group, which is the Fe^{2+} solution without the addition of the CADES sample; A_4 denotes the absorbance of the reaction solution containing Fe^{2+}, Ferrozine, and CADES; A_5 signifies the absorbance of the CADES sample in the absence of the Fe^{2+} solution.

3.5. Antibacterial Property

3.5.1. Antibacterial Zone

The antibacterial activity of CADES was evaluated against four bacterial strains (*Escherichia coli*, *Staphylococcus aureus*, *Pseudomonas aeruginosa,* and *Enterococcus faecalis*) using the standard filter paper agar diffusion method. The experimental protocol was executed as follows: First, a 50 μL aliquot of each bacterial suspension (1.0×10^8 CFU·mL^{-1}) was evenly spread across the surface of Luria-Bertani (LB) agar plates using a sterile spreader. Next, a sterile filter paper disc with a diameter of 9 mm was immersed entirely in the CADES solution. Using sterile forceps, the saturated filter paper disc was carefully placed at the center of the inoculated plate, ensuring complete and uniform contact between the disc and the agar surface. The inoculated plates were then incubated statically at 37 °C for 18 h. After the incubation period, the diameters of the inhibition zones (including the diameter of the filter

 doi:10.20944/preprints202507.0833.v1

paper disc) were measured and recorded. To guarantee the reproducibility and reliability of the results, the entire experiment was conducted in triplicate under identical experimental conditions.

3.5.2. Determination of the MIC of CADES

The MIC of CADES was determined using a standardized broth dilution method [48]. The experimental procedure was carried out as follows: Eleven sterile test tubes, numbered from 1 to 11, each containing 2 mL of sterilized LB medium. To initiate the dilution series, 2 mL of the CADES solution, with an initial concentration of 120 mg·mL^{-1} in sterile LB medium, was added to Tube 1 and mixed thoroughly. A serial two-fold dilution was then systematically performed. Specifically, 2 mL of the solution from Tube 1 was transferred to Tube 2, mixed well, and this process was repeated sequentially for each subsequent tube up to Tube 10. To maintain consistent volumes across all tubes, 2 mL of the solution was discarded from Tube 10. This meticulous procedure generated a series of CADES dilutions, ranging from 1:2 in Tube 1 to 1:1024 in Tube 10. Next, 100 μL of the bacterial suspension was inoculated into each of the test tubes numbered 1-10, as well as into a positive control tube. This inoculation was carried out to achieve a final bacterial concentration of 1.0×10^8 (CFU·mL^{-1}) in each tube, followed by thorough mixing to ensure uniform distribution of the bacteria. Afterward, all test tubes were sealed with rubber stoppers and incubated at 37 °C for 24 h. Bacterial growth was evaluated visually at the end of the incubation period. The MIC value was identified as the lowest concentration of CADES that completely inhibited visible bacterial growth, indicated by the absence of turbidity in the test tube. To ensure the validity and reliability of the experimental results, appropriate control samples were included. A positive control, containing bacteria but no CADES, was used to confirm normal bacterial growth under the experimental conditions. Additionally, a negative control, consisting of the medium without any bacteria, was included to rule out contamination and verify the sterility of the medium.

3.6. The Impact of CADES on the Germination Toxicity of Mung Beans

The composition of CADES can have a substantial impact on plant growth and development [49]. To evaluate the phytotoxic effects of CADES on mung bean (*Vigna radiata*) germination, ten distinct CADES formulations were diluted to 400-fold, 1200-fold, and 2000-fold, respectively, using deionized water. Deionized water was employed as the negative control to evaluate the germination toxicity of CADES on mung bean seeds. In the experimental design, sterilized petri dishes were lined with filter paper that was saturated with the respective CADES solutions. Ten uniformly sized, healthy mung bean seeds were aseptically placed in each dish and incubated at 30 °C in a controlled environment chamber. During the 7-day experimental period, 2 mL of the corresponding CADES solution was added daily to maintain optimal moisture levels. Germination parameters were systematically monitored. Daily root elongation was measured using cotton thread, and the germination rate was determined, with seeds considered germinated when sprouts exhibited a radicle emergence of $\geqslant 2$ mm. The phytotoxic effects were quantitatively evaluated through comparative analysis of germination rates across different treatment groups. The average germination rate (AGR%) and relative germination percentage (RGP%) were calculated according to the following formulas:

$$\mathrm{AGR}(\%) = \frac{\text{Germination Count}}{\text{The total number of pieces}} \times 100 \quad (6)$$

$$\mathrm{RGP}(\%) = \frac{\text{AGR following NADES treatment}}{\text{AGR following water treatment}} \times 100 \quad (7)$$

3.7. Extraction and Determination of Flavonoids from Walnut Green Peel

The powdered walnut green peel (60 mesh) was mixed with a CADES solution (containing 30% water) in a three-necked flask at a solid-liquid ratio of 1:30 (g·mL^{-1}). The mixture was stirred at 50 °C for 1 h to facilitate extraction. Subsequently, it was centrifuged at 12,000 rpm for 10 min, and the

 doi:10.20944/preprints202507.0833.v1

supernatant extract was carefully collected. The total flavonoid content (TFC) in the obtained extract was determined using the aluminum nitrate colorimetric method, as described by Wang et al. [50]. In detail, the extract was first diluted to an appropriate concentration. Then, 1.0 mL of the diluted solution was mixed with 300 μL of a 5% $NaNO_2$ solution. The mixture was shaken thoroughly and allowed to stand for 6 min. Following this, 300 μL of a 10% $Al(NO_3)_3$ solution was added, and the mixture was shaken again and incubated for another 6 min. Finally, 4 mL of a 4% NaOH solution was introduced, and the volume was adjusted to 10 mL with 70% ethanol. To ensure complete color development, the mixture was kept in the dark for 15 min. The absorbance of the solution was measured at 510 nm using a UV-Vis spectrophotometer. A standard calibration curve was constructed using rutin as the reference compound (Figure S3). The TFC was then calculated and expressed as milligrams of rutin equivalents per gram of the walnut green peel extract, recorded as mg RE·g^{-1} DW. To guarantee the reliability and accuracy of the results, all analyses were conducted in triplicate.

3.8. Statistical Analysis

The experiment was conducted at least three times, and the results were presented as mean ± standard deviation. Data analysis and graphical representation were carried out using OriginPro 2021 (OriginLab Co., USA) and GraphPad Prism 9 (GraphPad Software Inc., USA). One-way analysis of variance (ANOVA) was applied to assess statistical significance among three or more groups. $P \leq 0.05$ was considered statistically significant.

4. Conclusions

In this study, the physical properties of ten CADES, encompassing moisture content, polarity, electrical conductivity, pH, and viscosity, were systematically characterized. Beyond physical property analysis, their antioxidant and antibacterial activities, as well as potential toxicity effects on mung bean germination, were explored. The distinct molecular architectures and functional groups inherent to various carboxylic acids give rise to CADES with widely divergent physicochemical properties and biological activities. Notably, in the extraction of flavonoids from walnut green peel, the choline chloride/levulinic acid emerged as a standout performer, achieving an impressive extraction efficiency of 112.8 mg RE·g^{-1} DW. The innate antibacterial and antioxidant capabilities of CADES are critical determinants of the overall functionality of the extracts. This synergistic interaction not only amplifies the effectiveness of the extracted bioactive compounds but also endows the final products with multifaceted properties. These results underscore the significant potential of CADES-based extraction technology as a viable and promising method for isolating high-value natural products while enhancing their biological activity. This approach holds great promise for the sustainable utilization of natural resources and the development of innovative bioactive product formulations.

Supplementary Materials: The following supporting information can be downloaded at the website of this paper posted on Preprints.org, Figure S1: The standard curve of rutin; Figure S2: The inhibitory effect of ChCl/glycolic acid on different bacteria in culture dishes; Figure S3: The effects of different dilution ratios of ChCl/succinic acid on the germination toxicity of mung beans.

Author Contributions: Conceptualization, L.G.; methodology, L.G. and L.L.Y.; software, L.L.Y. and Q.L.C.; validation, L.G., L.L.Y. and Q.L.C.; formal analysis, L.G. and L.L.Y.; investigation, L.G. and L.L.Y.; resources, L.G., N.Z. and J.Z.; data curation, L.G., L.L.Y. and X.L.; writing—original draft preparation, L.G. and L.L.Y.; writing—review and editing, L.G.; visualization, L.G., X.L. and N.Z.; supervision, L.G. and J.Z.; project administration, L.G.; Funding acquisition, L.G. All authors have read and agreed to the published version of the manuscript.

Funding: This research was funded by the Project of Natural Science Research in Universities of Jiangsu Province (22KJB530004) and National Natural Science Foundation of China (22208030).

 doi:10.20944/preprints202507.0833.v1

Institutional Review Board Statement: Not applicable.

Informed Consent Statement: Not applicable.

Data Availability Statement: All data supporting the findings of this study are available within the paper.

Conflicts of Interest: The authors declare no conflicts of interest.

Abbreviations

The following abbreviations are used in this manuscript:

DESs	Deep eutectic solvents
CADESs	Carboxylic acid-based deep eutectic solvents
NADESs	Natural deep eutectic solvents
HBAs	Hydrogen bond acceptors
HBDs	Hydrogen bond donors
ILs	Ionic liquids
ChCl	Choline chloride
DPPH	2,2-diphenyl-1-picrylhydrazyl
ABTS	3-ethylbenzothiazoline-6-sulfonic acid
LB	Luria-Bertani
TFC	Total flavonoid content
MIC	Minimum inhibitory concentration
RGP	Relative germination rate
AGR	Average germination rate
HAT	Hydrogen atom transfer
mg RE·g^{-1} DW	mg Rutin Equivalent·g^{-1} Dry Weight

References

1. Smith, E.L.; Abbott, A.P.; Ryder, K.S. Deep eutectic solvents (DESs) and their applications. *Chem. Rev.* **2014**, *114*, 11060-11082. https://doi.org/10.1021/cr300162p.
2. Dong, Q.H.; Cao, J.; Chen, L.Y.; Cao, J.R.; Wang, H.M.; Cao, F.L.; Su, E.Z. Solubilization of phytocomplex using natural deep eutectic solvents: A case study of Ginkgo biloba leaves extract. *Ind. Crops. Prod.* **2022**, *177*, 114455. https://doi.org/10.1016/j.indcrop.2021.114455.
3. Fan, Y.C.; Luo, H.; Zhu, C.Y.; Li, W.J.; Wu, D.; Wu, H.W. Hydrophobic natural alcohols based deep eutectic solvents: Effective solvents for the extraction of quinine. *Sep. Purif. Technol.* **2021**, *275*, 119112. https://doi.org/10.1016/j.seppur.2021.119112.
4. Vanda, H.; Dai, Y.T.; Wilson, E.G.; Verpoorte, R.; Choi, Y.H. Green solvents from ionic liquids and deep eutectic solvents to natural deep eutectic solvents. *CR. Chim.* **2018**, *21*, 628-638. https://doi.org/10.1016/j.crci.2018.04.002.
5. Pan, Z.C.; Bo, Y.Y.; Liang, Y.H.; Lu, B.B.; Zhan, J.B.; Zhang, J.C.; Zhang, J.H. Intermolecular interactions in natural deep eutectic solvents and their effects on the ultrasound-assisted extraction of artemisinin from Artemisia annua. *J. Mol. Liq.* **2021**, *326*, 115283. https://doi.org/10.1016/j.molliq.2021.115283.
6. Chen, X.Q.; Li, Z.H.; Liu, L.L.; Wang, H.; Yang, S.H.; Zhang, J.S.; Zhang, Y. Green extraction using deep eutectic solvents and antioxidant activities of flavonoids from two fruits of *Rubia* species. *LWT-food. Sci. Technol*. **2021**, *148*, 111708. https://doi.org/10.1016/j.lwt.2021.111708.
7. Zhang, X.J.; Liu, Z.T.; Chen, X.Q.; Zhang, T.T.; Zhang, Y. Deep eutectic solvent combined with ultrasound technology: A promising integrated extraction strategy for anthocyanins and polyphenols from blueberry pomace. *Food. Chem*. **2023**, *422*, 136224. https://doi.org/10.1016/j.foodchem.2023.136224.
8. Hou, Y.J.; Wang, P.W.; Zhang, H.; Fan, Y.Y.; Cao, X.; Luo, Y.Q.; Li, Q.; Njolibimi, M.; Li, W.J.; Hong, B. A high-permeability method for extracting purple yam saponins based on ultrasonic-assisted natural deep eutectic solvent. *Food. Chem*. **2024**, *457*, 140046. https://doi.org/10.1016/j.foodchem.2024.140046.
9. Oliveira, I.; Sousa, A.; Ferreira, I.C.F.R.; Bento, A.; Estevinho, L.; Pereira, J.A. Total phenols, antioxidant potential and antimicrobial activity of walnut (*Juglans regia* L.) green husks. *Food. Chem. Toxicol*. **2008**, *46*, 2326-2331. https://doi.org/10.1016/j.fct.2008.03.017.
10. ZamaniBahramabadi, E.; Afshar, H.M.; Rezanejad, F. Chemical constituents of green peel of Persian walnut (*Juglans regia* L.) fruit. *Biomass. Convers. Bior*. **2024**, *14*, 27519-27524. https://doi.org/10.1007/s13399-022-03633-4.

 doi:10.20944/preprints202507.0833.v1

11. Karadaş F., Gültepe N. Effects of walnut (*Juglans regia*) green peel extract on growth performance and challenge to enteric redmouth disease (*Yersinia ruckeri*) in rainbow trout (*Oncorhynchus mykiss*). *Isr. J. Aquacult-Bamid*. **2025**, *77*, 90-96. https://doi.org/10.46989/001c.129419.
12. Moreira, C.D.; Santos, T.B.; Freitas, R.H.C.N.; Pacheco, P.A.F.; da Rocha, D.R. Juglone: A versatile natural platform for obtaining new bioactive compounds. *Curr. Top. Med. Chem*. **2021**, *21*, 2018-2045. https://doi.org/10.2174/1568026621666210804121054.
13. Liga, S.; Paul, C.; Peter, F. Flavonoids: Overview of biosynthesis, biological activity, and current extraction techniques. *Plants-Basel*. **2023**, *12*, 2732. https://doi.org/10.3390/plants12142732.
14. Okoye, C.O.; Jiang, H.F.; Wu, Y.F.; Li, X.; Gao, L.; Wang, Y.L.; Jiang, J.X. Bacterial biosynthesis of flavonoids: Overview, current biotechnology applications, challenges, and prospects. *J. Cell. Physiol*. **2024**, *239*, e31006. https://doi.org/10.1002/jcp.31006.
15. Dai, Y.T.; van Spronsen, J.; Witkamp, G.J.; Verpoorte, R.; Choi, Y.H. Natural deep eutectic solvents as new potential media for green technology. *Anal. Chim. Acta*. **2013**, *766*, 61-68. https://doi.org/10.1016/j.aca.2012.12.019.
16. Wei, J.H.; Zhao, G.J.; Wu, G.D.; Bo, Y.K.; Yang, D.; Guo, J.J.; Ma, Y.; An, M. An ultrasound-assisted extraction using an alcohol-based hydrophilic natural deep eutectic solvent for the determination of five flavonoids from *Platycladi Cacumen*. *Microchem. J*. **2024**, *198*, 110076. https://doi.org/10.1016/j.microc.2024.110076.
17. Rashid, R.; Wani, S.M.; Manzoor, S.; Masoodi, F.A.; Dar, M.M. Green extraction of bioactive compounds from apple pomace by ultrasound assisted natural deep eutectic solvent extraction: Optimisation, comparison and bioactivity. *Food. Chem*. **2023**, *398*, 133871. https://doi.org/10.1016/j.foodchem.2022.133871.
18. Meenu, M.; Bansal, V.; Rana, S.; Sharma, N.; Kumar, V.; Arora, V.; Garg, M. Deep eutectic solvents (DESs) and natural deep eutectic solvents (NADESs): Designer solvents for green extraction of anthocyanin. *Sustain. Chem. Pharm*. **2023**, *34*, 101168. https://doi.org/10.1016/j.scp.2023.101168.
19. Roda, A.; Santos, F.; Chua, Y.Z.; Kumar, A.; Do, H.T.; Paiva, A.; Duarte, A.R.C.; Held, C. Unravelling the nature of citric acid: l-arginine: water mixtures: the bifunctional role of water. *Phys. Chem. Chem. Phys*. **2021**, *23*, 1706-1717. https://doi.org/10.1039/d0cp04992a.
20. Wang, Y.B.; Li, Q.; Hong, H.; Yang, S.; Zhang, R.; Wang, X.Q.; Jin, X.; Xiong, B.; Bai, S.C.; Zhi, C.Y. Lean-water hydrogel electrolyte for zinc ion batteries. *Nat. Commun*. **2023**, *14*, 3890. https://doi.org/10.1038/s41467-023-39634-8.
21. Omar, K.A.; Sadeghi, R. Physicochemical properties of deep eutectic solvents: A review. *J. Mol. Liq*. **2022**, *360*, 119524. https://doi.org/10.1016/j.molliq.2022.119524.
22. Manasi, I.; Bryant, S.J.; Hammond, O.S.; Edler, K.J. Interactions of water and amphiphiles with deep eutectic solvent nanostructures. *Eutectic Solvents and Stress in Plants*. **2021**, *97*, 41-68. https://doi.org/10.1016/bs.abr.2020.09.002.
23. Shelembe, J.S.; Cromarty, D.; Bester, M.; Minnaar, A.; Duodu, K.G. Effect of acidic condition on phenolic composition and antioxidant potential of aqueous extracts from sorghum (*Sorghum bicolor*) bran. *J. Food. Biochem*. **2014**, *38*, 110-118. https://doi.org/10.1111/j.1745-4514.2012.00650.x.
24. Bashir, I.; Dar, A.H.; Dash, K.K.; Pandey, V.K.; Fayaz, U.; Shams, R.; Srivastava, S.; Singh, R. Deep eutectic solvents for extraction of functional components from plant-based products: A promising approach. *Sustain. Chem. Pharm*. **2023**, *33*, 101102. https://doi.org/10.1016/j.scp.2023.101102.
25. Pinho, M.R.; Lima, A.S.; Oliveira, G.D.R.; Liao, L.M.; Franceschi, E.; da Silva, R.; Cardozo, L. Choline chloride- and organic acids-based deep eutectic solvents: Exploring chemical and thermophysical properties. *J. Chem. Eng. Data*. **2024**, *69*, 3403-3414. https://doi.org/10.1021/acs.jced.3c00706.
26. Yusof, R.; Abdulmalek, E.; Sirat, K.; Rahman, M.B.A. Tetrabutylammonium bromide (TBABr)-based deep eutectic solvents (DESs) and their physical properties. *Molecules*. **2014**, *19*, 8011-8026. https://doi.org/10.3390/molecules19068011.
27. Maciel, E.N.; Almeida, S.K.C.; da Silva, S.C.; de Souza, G.L.C. Examining the reaction between antioxidant compounds and 2,2-diphenyl-1-picrylhydrazyl (DPPH) through a computational investigation. *J. Mol. Model*. **2018**, *24*, 218. https://doi.org/10.1007/s00894-018-3745-1.
28. Munteanu, I.G.; Apetrei, C. Analytical methods used in determining antioxidant activity: A review. *Int. J. Mol. Sci*. **2021**, *22*, 3380. https://doi.org/10.3390/ijms22073380.
29. Dai, J.; Liu, Y.M.; Li, J.; Lu, Z.Y.; Yang, W.S. Phenanthroline method for quantitative determination of surface carboxyl groups on carboxylated polystyrene particles with high sensitivity. *Surf. Interface. Anal*. **2009**, *41*, 577-580. https://doi.org/10.1002/sia.3065.

 doi:10.20944/preprints202507.0833.v1

30. Bedair, H.M.; Samir, T.M.; Mansour, F.R. Antibacterial and antifungal activities of natural deep eutectic solvents. *Appl. Microbiol. Biot*. **2024**, *108*, 198. https://doi.org/10.1007/s00253-024-13044-2.
31. Wen, Q.; Chen, J.X.; Tang, Y.L.; Wang, J.; Yang, Z. Assessing the toxicity and biodegradability of deep eutectic solvents. *Chemosphere*. **2015**, *132*, 63-69. https://doi.org/10.1016/j.chemosphere.2015.02.061.
32. Taysun, M.B.; Sert, E.; Atalay, F.S. Effect of hydrogen bond donor on the physical properties of benzyltriethylammonium chloride based deep eutectic solvents and their usage in 2-ethyl-hexyl acetate synthesis as a catalyst. *J. Chem. Eng. Data*. **2017**, *62*, 1173-1181. https://doi.org/10.1021/acs.jced.6b00486.
33. Silva, J.M.; Silva, E.; Reis, R.L.; Duarte, A.R.C. A closer look in the antimicrobial properties of deep eutectic solvents based on fatty acids. *Sustain. Chem. Pharm.* **2019**, *14*, 100192. https://doi.org/10.1016/j.scp.2019.100192.
34. Martínez, G.M.; Townley, G.G.; Martínez-Espinosa, R.M. Controversy on the toxic nature of deep eutectic solvents and their potential contribution to environmental pollution. *Heliyon.* **2022**, *8*, e12567. https://doi.org/10.1016/j.heliyon.2022.e12567.
35. Thinh, B.B.; Thin, D.B.; Ogunwande, I.A. Chemical composition, antimicrobial and antioxidant properties of essential oil from the leaves of *Vernonia volkameriifolia* DC. *Nat. Prod. Commun*. **2024**, *19*, 1934578X241239477. https://doi.org/10.1177/1934578X241239477.
36. Oke, E.A.; Ijardar, S.P. Advances in the application of deep eutectic solvents based aqueous biphasic systems: An up-to-date review. *Biochem. Eng. J*. **2021**, *176*, 108211. https://doi.org/10.1016/j.bej.2021.108211.
37. Li, P.F.; Liu, C.L.; Luo, Y.; Shi, H.N.; Li, Q.; PinChu, C.E.; Li, X.J.; Yang, J.L.; Fan, W. Oxalate in plants: Metabolism, function, regulation, and application. *J. Agric. Food. Chem*. **2022**, *70*, 16037-16049. https://doi.org/10.1021/acs.jafc.2c04787.
38. Atilhan, M.; Costa, L.T.; Aparicio, S. On the behaviour of aqueous solutions of deep eutectic solvents at lipid biomembranes. *J. Mol. Liq*. **2017**, *247*, 116-125. https://doi.org/10.1016/j.molliq.2017.09.082.
39. Stanisz, M.; Stanisz, B.J.; Cielecka-Piontek, J. A comprehensive review on deep eutectic solvents: Their current status and potential for extracting active compounds from adaptogenic plants. *Molecules*. **2024**, *29*, 4767. https://doi.org/10.3390/molecules29194767.
40. Wu, C.Y.; Wang, B.R.; Han, S.Y.; Zhang, Y.H.; Mu, Z.S. Extraction of hydroxy safflower yellow A and anhydroxysafflor yellow B from safflower florets using natural deep eutectic solvents: Optimization, biological activity and molecular docking. *Food. Biosci*. **2025**, *68*, 106418. https://doi.org/10.1016/j.fbio.2025.106418.
41. Hao, Y.; Pei, F.X.; Huang, J.J.; Li, G.Z.; Zhong, C.L. Application of deep eutectic solvents on extraction of flavonoids. *J. Sep. Sci*. **2024**, *47*, 2300925. https://doi.org/10.1002/jssc.202300925.
42. Chen, J.N.; Li, Y.; Wang, X.P.; Liu, W. Application of deep eutectic solvents in food analysis: A review. *Molecules*. **2019**, *24*, 4594. https://doi.org/10.3390/molecules24244594.
43. Airouyuwa, J.O.; Mostafa, H.; Ranasinghe, M.; Maqsood, S. Influence of physicochemical properties of carboxylic acid-based natural deep eutectic solvents (CA-NADES) on extraction and stability of bioactive compounds from date (*Phoenix dactylifera* L.) seeds: An innovative and sustainable extraction technique. *J. Mol. Liq.* **2023**, *388*, 122767. https://doi.org/10.1016/j.molliq.2023.122767.
44. Ogihara, W.; Aoyama, T.; Ohno, H. Polarity measurement for ionic liquids containing dissociable protons. *Chem. Lett.* **2004**, *33*, 1414-1415. https://doi.org/10.1246/cl.2004.1414.
45. Sarikurkcu, C.; Kirkan, B.; Ozer, M.S.; Ceylan, O.; Atilgan, N.; Cengiz, M.; Tepe, B. Chemical characterization and biological activity of *onosma gigantea* extracts. *Ind. Crop. Prod.* **2018**, *115*, 323-329. https://doi.org/10.1016/j.indcrop.2018.02.040.
46. Jia, M.Z.; Fu, X.Q.; Deng, L.; Li, Z.L.; Dang, Y.Y. Phenolic extraction from grape (*Vitis vinifera*) seed via enzyme and microwave co-assisted salting-out extraction. *Food Biosci.* **2021**, *40*, 100919. https://doi.org/10.1016/j.fbio.2021.100919.
47. Papuc, C.; Crivineanu, M.; Goran, G.; Nicorescu, V.; Durdun, N. Free radicals scavenging and antioxidant activity of European Mistletoe (*Viscum album*) and European Birthwort (*Aristolochia clematitis*). *Rev. Chim-Bucharest.* **2010**, *61*, 619-622.
48. Dlugosz, O.; Chmielowiec-Korzeniowska, A.; Drabik, A.; Tymczyna, L.; Banach, M. Bioactive selenium nanoparticles synthesized from propolis extract and quercetin based on natural deep eutectic solvents (NDES). *J. Clust. Sci.* **2023**, *34*, 1401-1412. https://doi.org/10.1007/s10876-022-02306-6.

 doi:10.20944/preprints202507.0833.v1

49. Dai, Y.T.; Varypataki, E.M.; Golovina, E.A.; Jiskoot, W.; Witkamp, G.J.; Choi, Y.H.; Verpoorte, R. Natural deep eutectic solvents in plants and plant cells: In vitro evidence for their possible functions. *Eutectic Solvents and Stress in Plants.* **2021**, *97*, 159-184. https://doi.org/10.1016/bs.abr.2020.09.012.
50. Wang, Z.W.; Wang, D.D.; Fang, J.X.; Song, Z.X.; Geng, J.M.; Zhao, J.F.; Fang, Y.F.; Wang, C.T.; Li, M. Green and efficient extraction of flavonoids from *perilla frutescens* (l.) britt. Leaves based on natural deep eutectic solvents: Process optimization, component identification, and biological activity. *Food. Chem.* **2024**, *452*, 139508. https://doi.org/10.1016/j.foodchem.2024.139508.